

## PERFORMANCE EVALUATION OF NANOFLUID ON PARABOLIC TROUGH SOLAR COLLECTOR

by

**Gopalsamy VIJAYAN<sup>a\*</sup> and Karunakaran RAJASEKARAN<sup>b</sup>**

<sup>a</sup> Department of Mechanical Engineering,  
Anna University-Chennai, Tamilnadu, India

<sup>b</sup> Department of Mechanical Engineering, UCE-Kanchipuram,  
Anna University-Chennai, Tamilnadu, India

Original scientific paper  
<https://doi.org/10.2298/TSCI180509059G>

*In the present work, the performance of aluminum oxide and deionized water nanofluid used as heat transfer fluid on a parabolic trough solar collector system with hot water generation tank is evaluated. The parabolic trough solar collector is developed using easily and locally accessible materials. Five different concentrations of aluminum oxide and deionized water based nanofluid from 0.5-2.5% is prepared by the magnetic stirrer initially and then the mixture is subjected to ultrasonication process to break aggregates with the absence of surfactant. The prepared nanofluids are allowed to flow through the absorber which is located at a focal point of the solar collector. The performance of nanofluid is compared with pure deionized water. The test is conducted from 8.00 a. m. to 16.00 p. m. daily in the whole length of the test span. The heat transfer fluid is allowed to flow at a mass-flow rate of 0.020 kg/s and 0.09246 m/s velocities. The maximum solar radiation is 821 W/m<sup>2</sup>, and maximum efficiency is observed at noon time 60.41% for deionized water and 60.49% for 2.5% volumetric fraction of alumina nanofluid. The efficiency enhancement was 3.90% than deionized water. The influence of the critical parameter on the performance is also examined.*

Key words: *parabolic trough solar collector; alumina, deionized water, nanofluid, volume fraction, rim angle*

### Introduction

The parabolic trough solar concentrator system is used for unique fields such as power production [1, 2], steam and hot water generation for the domestic purpose [3, 4]. The possibilities of producing hot water using parabolic trough solar collector (PTSC) were discussed. Research work so far done proves that the PTSC holds good for hot water generation when compared with the non-concentrating type of solar collector. The concentrated type solar collector of conical geometry was also used for hot water production [5]. The PTSC was used for domestic power generation purpose using the stirling cycle, where water was used as a heat transfer fluid [6]. Many researchers investigated the performance of nanofluid on parabolic trough concentrator, instead of using water as a working fluid and they compared the performance [7]. Nanosized solid particles mixed in liquid, are known as nanofluid, was used in the solar collector. Many research works were carried out to analyze the

\* Corresponding author, e-mail: [viji\\_laker@yahoo.co.in](mailto:viji_laker@yahoo.co.in)

performance of nanofluid of various types and volume fractions on PTSC. They detailed the list of various heat transfer fluids such as synthetic oil, therminol VP-I, nitrate salt: 395 °C, ionic liquid: 459 °C, CO<sub>2</sub>: 480 °C, and sulphur: 490 °C which can be used depending upon the working temperature, operation aspects, storage aspects, safety aspects, and cost on parabolic trough solar thermal power plant [8]. The therminol VP-I, nitrate molten salt, sodium liquid, air, carbon monoxide, pressurized water, and helium can also be applied as heat transfer fluids [9]. The author constructed a standard pilot model of parabolic trough collector with four kinds of receiver namely black painted vacuumed steel pipe, bare copper tube coated with black chrome coating, non-evacuated glass tube and vacuumed copper tube with a black coating. The carbon nanotubes of 0.2% and 0.3% volume fraction were dispersed into the oil to use as working fluid [10-12]. The author used distilled water based multi-wall carbon nanotube and potassium persulfate as an oxidant. The nanofluid was prepared with the volume fractions of 49.9-50.1 mg per litre of distilled water for balancing pumping power. The collector efficiency enhances from 54-73% when using multiwall carbon nanotubes in a glass tube receiver and operating temperature increases from ambient to 80 °C [13]. The author analyzed the forced convection heat transfer of CuO-water and Al<sub>2</sub>O<sub>3</sub>-water nanofluid while subjected to flow through the receiver tube of the PTSC numerically [14]. The author used Monte Carlo ray tracing (MCR) method to investigate the effect of rotational and irrotational of the LS-2 Luz collector on fluid outlet temperature and heat gain, where syltherm-800 was used as heat transfer fluid. The result proved the rotation of collector has a positive effect [15].

Many authors analyzed and compared the experimental output with the results obtained from the simulation and other analysis techniques. Numerical [16-19], experimental [20, 21], simulation, numerical [22], analytical [23], modelling, heat transfer analysis work [16, 24] and modelling cum optimization [25, 26] were carried out for the purpose of evaluating their results. The author carried out the modelling of PTSC with a well-mixed hot water storage tank. They developed the model, and its results were verified with experimental work. The hot water temperature deviation between predicted and actual is 9.59% only [27]. The author analyzed the solar dish collector both optically and thermally by SolidWorks software. Maximum optical efficiency is obtained at 2.1 m focal length and exergetic efficiency is varied from 4-15% depending upon the inlet water temperature [28]. They investigated the effect of solar radiation on performance parameters of PTSC over the test period [29]. The author developed two hybrid solar collectors with the photovoltaic panel, one fixed above the absorber and other located on the absorber itself to investigate the conversion ability of solar radiation into heat and/or electricity [30]. Extensive research work in synthesizing of distinctive types of nanofluid at various volume fractions either by one step or two-step method was done. Properties of nanofluid were evaluated, and the performance enhancement was analyzed while using in the absorber of the PTSC [31-33].

In this present work, the performance of the PTSC is investigated experimentally while the Al<sub>2</sub>O<sub>3</sub>/deionized (DI) water nanofluid of various volume fractions is subjected to flow through it. Both the fabrication of PTSC and preparation of alumina nanofluid are done in the lab. Most of the work carried out so far on PTSC, using nanofluid as heat transfer fluid was with shielded type receiver and incurred a high cost. Only very few works were done on the unshielded receiver with nanofluid. So an attempt has been made to develop the low-cost unshielded receiver type PTSC by utilizing the locally available materials.

## Experimental platform

### Parabolic trough solar collector system

The present research work includes two parts:

- fabrication of a PTSC and
- preparation of Al<sub>2</sub>O<sub>3</sub> and DI water nanofluid. Fabrication of the PTSC system and preparation of Al<sub>2</sub>O<sub>3</sub>/DI water nanofluid are done in the lab.

A new low-cost parabolic trough solar concentrator with hot water production system is developed for this research work. The total cost of the system is around 390 USD. The complete system includes:

- aperture-to reflect the solar radiation,
- absorber-to absorb the radiation reflected from the reflector (aperture) surface and transferring the heat energy to heat transfer medium,
- heat energy storage system-to transfer the heat energy of nanofluid to water through heat exchanger which is kept in the heat energy storage tank,
- nanofluid tank-to store the nanofluid, and
- mini submersible pump-to circulate nanofluid which is placed inside the nanofluid tank.

The parabolic geometry [34, 35] is developed by an eq. (1) and the calculated rim angle is 73.74° as shown in fig. 1. The parabolic curvature is fabricated by mild steel sheet as per the accurately calculated value. The locally available plane mirror,  $\tau = 0.97$ , of striped shape with reflectivity is fixed on the curvature to complete the reflector part, which reflects the incident solar rays equal to the angle of incidence. The selection of the reflector is based on the availability, reflectivity, and cost. The sketch of the experimental set-up is shown in fig. 2, and the detailed specifications are given tab. 1.

$$X^2 = 4fy \quad (1)$$

The collector is kept on an open terrace (Longitude: 79.3881° E, Latitude: 10.9617 ° N) oriented north-south direction and tracked manually in east-west. Tracking was monitored for every 5 minutes in such a way to receive maximum radiation. The test was carried out from 8.00 a. m. to 4.00 p. m. every test day for six values of concentration and 0.02 kg/s of mass-flow rate. The copper tube is selected as the receiver due to its high thermal conductivity, and it is painted black to absorb the solar radiation utmost. The receiver is aligned at a calculated focal point to face the solar radiation from the reflector surface always. Both the absorber and aperture are supported by a sturdy mild steel structure. The PTSC is oriented



Figure 1. Parabolic structure

Table 1. Specifications of PTSC

Parameter	Design value
Collector length [mm]	1200
Collector width [mm]	900
Absorber inner diameter [mm]	16.6
Absorber outer diameter [mm]	17.2
Aperture area [m <sup>2</sup> ]	1.08
Focus length [mm]	300
Mirror radius [°]	474
Local mirror radius [°]	346.5
Rim angle [°]	73.74
Minimum image diameter [mm]	4.418
Energy storage tank [L]	15
Nanofluid tank [L]	5
Mass-flow rate [kgs <sup>-1</sup> ]	0.020
Concentration ratio	16.34
Reflectivity	0.97
Intercept factor	0.91
Absorptance	0.90

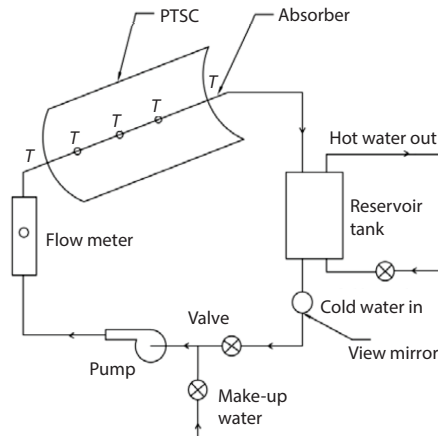


Figure 2. Sketch of PTSC

absorber surface temperature, ambient temperature, and heat energy storage tank fluid temperature. A mini submersible pump kept in the nanofluid tank is used to circulate the nanofluid continuously through the receiver, heat energy storage tank and finally to the nanofluid tank at a defined mass-flow rate, to complete the fluid circuit. The rotameter is connected at the entry side of the receiver to control the mass-flow rate of nanofluid.

#### Preparation of nanofluid

Nanofluid is prepared by a two-step method. In this method first nanoparticles are prepared then it is mixed with the base fluid. In our work, the  $\text{Al}_2\text{O}_3$  nanoparticles are bought from M/s. Alfa Asear, and it is mixed with DI water without surfactant presence. The properties of nanoparticle are given in tab. 2. The required quantity of nanoparticle for preparing the



Figure 3. Magnetic stirrer

Table 2. Specifications of nanoparticle

Chemical name	Aluminum oxide	Appearance	White
Formula	$\text{Al}_2\text{O}_3$	Surface area	$32\text{-}40 \text{ m}^2\text{g}^{-1}$
Make	Nanodur	Density	$3.72 \text{ gcm}^{-3}$
Phase	Solid	Melting point	$2045 \text{ }^\circ\text{C}$
Shape	Sphere	Boiling point	$2980 \text{ }^\circ\text{C}$
Form	Powder	$C_p$	$765 \text{ Jkg}^{-1}\text{K}^{-1}$
Purity	99.5%	$K$	$40 \text{ Wm}^{-1}\text{K}^{-1}$

nanofluid is calculated as per the eq. (2) and weight of the particles required per 1000 ml presented in tab. 3. Actually, it is the ratio of the volume of nanoparticle,  $V_{np}$ , to the sum of the nanoparticle volume and the base fluid volume,  $V_{bf}$ . The figs. 3 and 4 show the nanofluid preparation equipment. The calculated quantity of alumina particles is weighed by an electronic weighing machine. First, the alumina nanoparticles are diluted in DI water using magnetic stirrer, which is operated at a speed of 500 rpm for the period of 30 minutes. Then the mixture is subjected to ultrasonication process for 60 minutes, It is an approved and commonly used technique for nanofluid preparing. Various volume fractions of nanofluid are prepared such as 0.5, 1.0, 1.5, 2.0, and 2.5%, each of 5000 ml per concentration, to act as heat transfer fluid and to complete the nanofluid cycle.



Figure 4. Ultrasonic bath



Figure 5. Experimental set-up

$$W_{np} = \left[ \frac{V_{np}}{V_{np} + V_{bf}} \right] \quad (2)$$

Table 3. Weight of np/1000ml

Concentration [%]	Weight [g]
0.5	18.6
1.0	37.2
1.5	55.8
2.0	74.4
2.5	93.0

*Performance tests*

The experimental work is carried out on the collector system as shown in fig. 5, and the efficiency of the system is determined from the obtained values. The instantaneous efficiency for different solar radiation intensity, ambient temperature, nanofluid inlet temperature, and wind velocity are calculated. The absorbed solar radiation depends on the reflectivity of aperture material, therefore, the collector surface having good reflectance property will reflect almost all the radiation which is falling on the surface and it can be calculated [36-38] as per eq. (3). Both wind loss and radiation loss influences the heat coefficient and can be calculated

by eq. (4). Wind loss coefficient is affected by wind velocity, ambient temperature, and absorber surface temperature which are dominating parameters:

$$S = I_b R_b \rho \gamma (\tau \alpha) + I_b R_b (\tau \alpha) \left( \frac{D_o}{W + D_o} \right) \quad (3)$$

$$U_l = \left[ \frac{1}{h_w} + \frac{1}{h_r} \right]^{-1} \quad (4)$$

For the nanofluid-flowing inside the tube, first, the bulk mean temperature is calculated. Then, the properties such as density, kinematic viscosity, dynamic viscosity, specific heat, Prandtl number, and thermal conductivity are to be taken from their thermophysical property data at bulk mean temperature which is calculated experimentally. To confirm whether the flow is laminar or turbulent, the value of Reynolds number is calculated. If the value of  $Re < 2300$ , then the flow is laminar so that the flow is coming under fully developed hydrodynamic and thermal profile mode. Therefore,  $Nu = 3.7$  is considered for constant wall temperature [34]. If the value is in the range of  $2300 < Re < 5 \cdot 10^6$  and  $0.5 < Pr < 2000$ , then the nanofluid-flowing

inside the receiver tube ensures fully developed turbulent flow region. The eqs. (5) and (6) represented by Gnielinski is used to calculate the friction factor and Nusselt number for turbulent flow:

$$f = [1.58 \ln(\text{Re}) - 3.28]^{-2} \quad (5)$$

$$\text{Nu} = \frac{\left(\frac{f}{2}\right)(\text{Re} - 1000)\text{Pr}}{1.0 + 12.7\left(\sqrt{\frac{f}{2}}\right)(\text{Pr}^{2/3} - 1)} \quad (6)$$

There is no variation in the receiver tube dimension and its thermal conductivity, then the heat loss coefficient and inside heat transfer coefficient dominates the overall heat loss coefficient as per the eq. (7):

$$U_o = \left[ \left(\frac{1}{U_i}\right) + \left(\frac{D_o}{D_i h_{fi}}\right) + \left(\frac{D_o}{2K_r}\right) \ln\left(\frac{D_o}{D_i}\right) \right]^{-1} \quad (7)$$

The actual useful heat gain is the difference between useful heat gain and total heat loss and is determined by the eq. (8) and the instantaneous collector efficiency is proportional to the actual useful heat gain available and it is the ratio of useful heat gain and heat available from the aperture area. It can be determined from eq. (9).

$$Q_u = F_R A_a \left( S - \frac{1}{CR} \right) U_o (T_{fi} - T_a) \quad (8)$$

$$\eta_{ms} = \left[ \frac{Q_u}{I_b R_b WL} \right] \quad (9)$$

Now the optical efficiency is determined for the various incident angle of solar radiation by eq. (9). The optical efficiency,  $\eta_{opt}$ , only depends on the reflectivity of aperture material,  $\rho$ , intercept factor,  $\gamma$ , and the transmittance-absorptance product of the receiver,  $\tau\alpha$ . Both the incident angle modifier and end loss were also taken in to account as shown in eq. (10) while calculating the optical efficiency.

$$\eta_{opt} = (\rho\gamma\tau\alpha)K(\theta)(X_{\text{endloss}}) \quad (10)$$

The transmittance parameter can be omitted due to unshielded type receiver. The inlet temperature of nanofluid and an outlet temperature of nanofluid, ambient temperature, and the water temperature are observed using PT-100 resistance temperature detector. The solar power meter, vane type anemometer, and rotameter are used to measure the beam radiation, wind speed, and mass-flow rate, respectively, along with the instrument details in tab. 4. Each concentration was tested for three days. Before charging the next concentration, the existing nanofluid is fully drained. To complete the cleaning process the test run was conducted with de-ionized water, and then the system is kept in ideal condition. All these parameters are observed at every five minutes time interval. The parametric values measured using the instruments discussed here have not deviated over the limit specified by the ASHRAE standard which confirms that the experimental works are under steady-state condition and considering the uncertainty of the measuring instruments, in mind, the experimental error was calculated as 2.06%.

**Table 4. Details of instrumentation**

Parameter	Instrument	Model	Accuracy
Solar radiation	Solar power meter	TM 207	$\pm 10 \text{ Wm}^{-2}$
Wind speed	Vane probe anemometer	AVM 07	$\pm 2\% + 0.1 \text{ ms}^{-1}$
Ambient temperature			$\pm 0.5 \text{ }^\circ\text{C}$
Temperature	RTD	PT 100	$\pm [0.15 + 0.02(t)] \text{ }^\circ\text{C}$

**Results and discussion**

The variation of ambient temperature, bulk mean temperature and surface temperature during the whole testing period is shown in fig. 6. It attained highest receiver temperature of  $139.82 \text{ }^\circ\text{C}$ , and the bulk mean temperature at that time is  $42.67 \text{ }^\circ\text{C}$  which is the maximum value of particular test day hour. These three temperatures are purely depended on solar radiation and it increased with radiation and wind velocity. Low wind velocity and high solar radiation offered the fruitful result in terms of higher receiver temperature which is the reason for the increase in the outlet temperature of the nanofluid. But at the same time, its heat transfer rate is decreased due to increase the inlet temperature of the nanofluid where the temperature difference between the inlet and outlet of flowing fluids (deionized water and alumina nanofluid) is steadily increased from 8.00-11.00 a. m., and then there is a fluctuation up to 4.00 p. m. Both the inlet and an outlet temperature of nanofluid are varied depending upon solar radiation as shown in fig. 7. Figure 8 shows the maximum temperature difference ( $23.3 \text{ }^\circ\text{C}$ ) which is reached at 11.00 a. m. when the radiation is maximum.

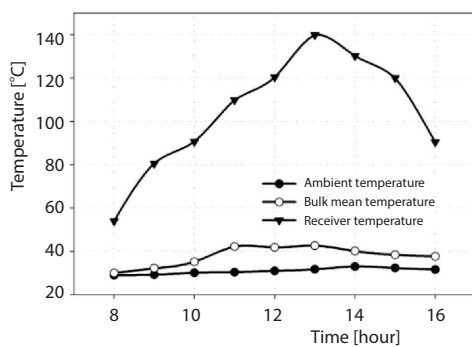


**Figure 6. Temperatures with time**

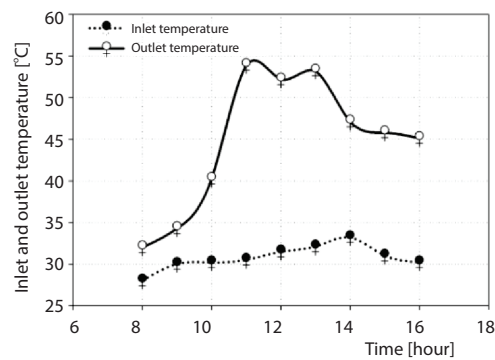


**Figure 7. The inlet/outlet temperature variations**

Wind loss coefficient mainly depended on the wind speed and the thermal properties of air at ambient temperature. The variation of wind speed with respect to test time is shown in fig. 9. The wind velocity is proportional to Reynolds number which has a direct effect on the Nusselt number. Wind loss coefficient increased with increased wind speed. Up to 5.6 m/s speed, the wind power falls under the category of class 1 level and it is called poor wind. During the whole test period, the air velocity does not reach beyond this poor wind class. Radiation heat loss depends on the emissivity of the receiver material, ambient temperature, and receiver temperature which are the three parameters retaining the honest influence on radiation heat loss. The heat loss coefficient, radiation heat loss, and wind loss coefficient were fluctuating and reached the maximum values of 7.026, 8.134, and  $51.32 \text{ W/m}^2\text{K}$ , respectively as shown in

fig. 10. Heat loss from the collector system to the surrounding atmosphere by all three modes of heat transfer are known as outside heat transfer coefficient, and it can be calculated by the product of heat loss coefficient and the temperature difference of surface-ambient.

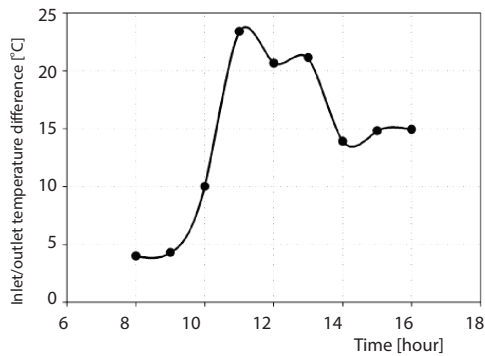


Figure 8. The inlet/outlet temperature difference

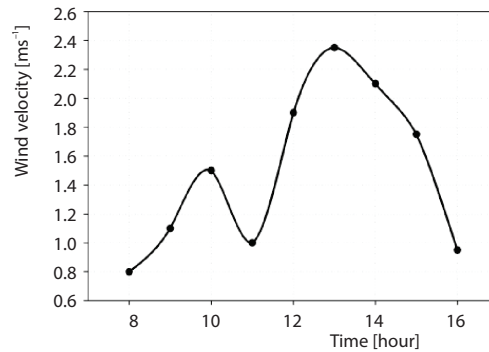


Figure 9. Variation of wind speed

The variation of inside heat transfer coefficient with bulk mean temperature for minimum and maximum fraction of nanofluid is shown in fig. 11. The trend showed that the heat transfer coefficient is gradually increased and reached the maximum value of  $634.5 \text{ W/m}^2\text{K}$  at 1.00 p. m. where the bulk mean temperature is  $42.67 \text{ }^\circ\text{C}$ . The optical efficiency also started from 31.57% minimum at 8.00 a. m. and it is gradually increased to a maximum of 60.75% at 12.00 noon. It depends on the optical property of reflector and the intercept factor. For the maximum beam radiation of  $821 \text{ W/m}^2$ , the total solar flux is  $554.45 \text{ W/m}^2$ , but the highest value is  $587.28 \text{ W/m}^2$  at 2.00 p. m., where the receiver temperature is  $130.20 \text{ }^\circ\text{C}$ , as shown in fig. 12. Solar flux is the quantity of solar radiation absorbed after overcoming the hurdles such as tilt factor, intercept factor, optical properties, receiver properties, and width of the aperture. The beam radiation, solar flux, and receiver temperature have increased positively up to noon time then gradually decreased in the opposite manner.

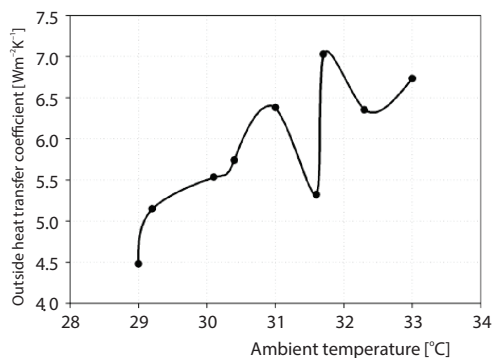


Figure 10. Outside heat transfer coefficient

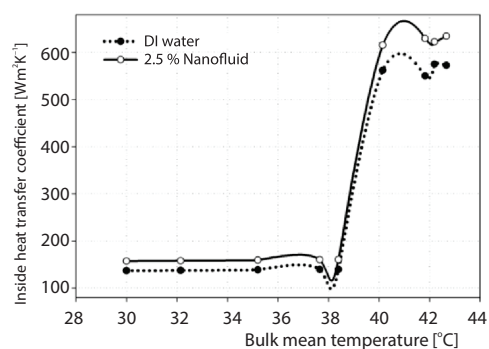


Figure 11. Inside heat transfer coefficient

The total loss coefficient range for the heat transfer fluid such as DI water and alumina nanofluid uniformly increased from  $30 \text{ }^\circ\text{C}$  ( $4.342 \text{ W/m}^2\text{K}$ ) to  $41.8 \text{ }^\circ\text{C}$  ( $6.31 \text{ W/m}^2\text{K}$ ) as shown in fig. 13. This loss coefficient between the two heat transfer fluids is in the range of negligible quantity. The flow slowly moved towards the turbulent type from the bulk mean temperature of  $40 \text{ }^\circ\text{C}$  (11.00 a. m.). This rule is applicable for the given inner diameter (16.6

mm) of the receiver, mass-flow rate (0.020 kg/s) of fluid and velocity of heat transfer fluid (0.09246 m/s). The variation in temperature to the assumed turbulent flow depends on the internal diameter of the receiver, mass-flow rate, and fluid velocity.

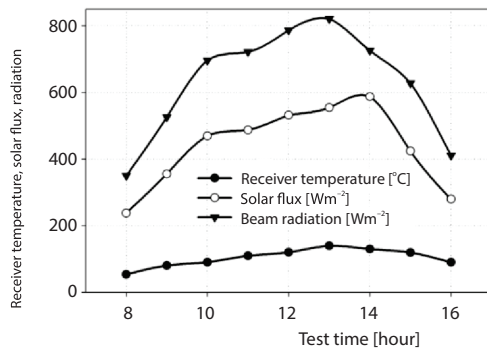


Figure 12. Parameters variation

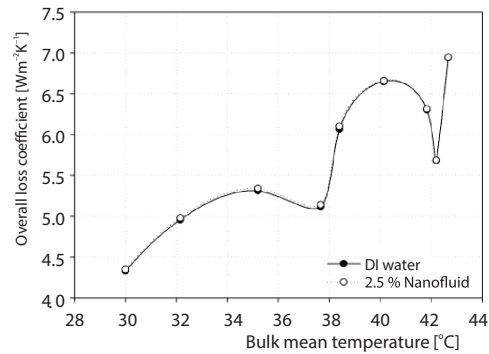


Figure 13. Overall loss coefficients

The useful heat gain increased with respect to the nanofluid concentration. The variation between the inlet temperature of heat transfer medium and ambient temperature had an influence [39] on useful heat gain. The effect of volume fraction on useful heat gain is given in fig. 14. The maximum possible useful heat gain can be obtained when the total collector system is maintained at the entry temperature of heat transfer fluid. As per the calculated data, the enhancement of collector efficiency is proportional to nanofluid volume fraction as shown in fig. 15. The graph is plotted based on the average efficiency of the whole day for DI water and 2.5% concentrations. This demonstrates a very good relation between nanofluid concentration and collector efficiency. The maximum instantaneous efficiency reached is 59.68% for 2.5% concentration. The collector efficiency increased parallel to the concentration of nanofluid. The thermal conductivity of nanofluid is higher than DI water. At the same time, the specific heat decreased with increased concentration.

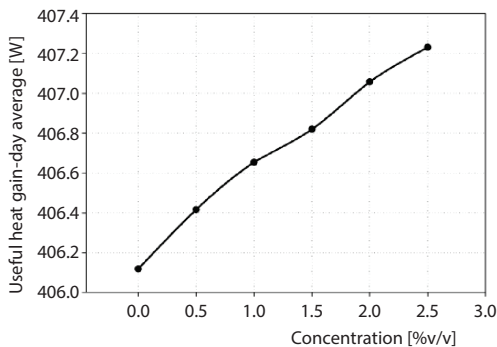


Figure 14. Useful heat gain

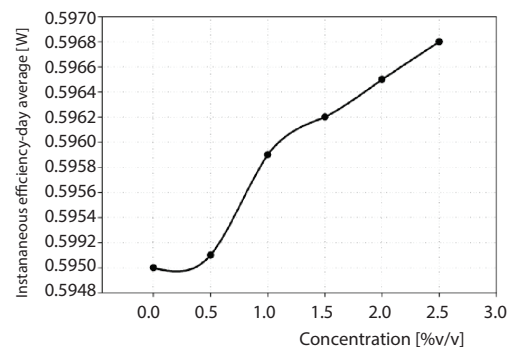


Figure 15. Efficiency on day average

The variation of instantaneous collector efficiency between the DI water and nanofluid of 2.5% concentration is shown in fig. 16. The heat transfer fluids are under turbulent region from 10.00 a. m. to 3.00 p. m. and the rest of the test times are in the laminar flow region. The instantaneous collector efficiency slowly increased from 10.00 a. m. to 3.00 p. m. due to its turbulent flow nature than other test times. The mass-flow rates and concern velocities keep the fluid in the laminar region up to a certain temperature level. The calculated bulk mean tem-

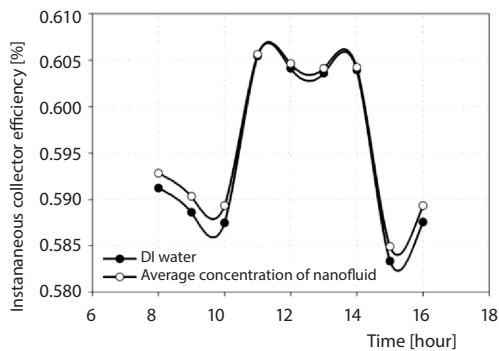


Figure 16. Efficiency of 0% and 2.5%

perature for the mass-flow rate is 40 °C. The bulk mean temperature of the heat transfer fluid is not allowed to increase beyond the given level to keep the flowing fluid in the laminar region. Due to the increase in the inside heat transfer coefficient at the turbulent region, the collector efficiency is enhanced. The variation in efficiency was observed for the defined heat transfer fluid from 12.00 noon 1.00 p.m. The instantaneous efficiency slowly decreased from 8.00 a. m. to 10.00 a. m. and then it reached to precise position due to its turbulent flow nature where the inside heat transfer rate is high, 634.5 W/m<sup>2</sup>K. By 11.00 a. m. the PTSC reached the high collector efficiency of 60.58%.

## Conclusion

In the present work, the low-cost PTSC with hot water generation system for domestic purpose is designed and fabricated. The various volume fractions of Al<sub>2</sub>O<sub>3</sub>/DI water such as from 0.5-2.5% are prepared by two-step method using magnetic stirrer and sonication. The experiments are carried out for nine hours from 8.00 a. m. to 4.00 p. m. of test day. The Al<sub>2</sub>O<sub>3</sub> nanofluid is used as a heat transfer medium and it is allowed to flow through the copper receiver pipe. The maximum beam radiation is 821 W/m<sup>2</sup> and the average is 629.67 W/m<sup>2</sup>. The coefficient of wind loss, radiation loss, heat loss, overall loss, inside heat transfer, friction factor at the time of turbulent flow, collector efficiency factor, solar flux, useful heat gain, heat removal factor, collector capacitance factor and finally collector efficiency are also calculated based on day average as well as hourly basis. The instantaneous efficiency is increases parallel to useful heat gain. The efficiency of the collector and maximum heat gain is 59.68% and 467.231 W for 2.5% concentration on day average basis. On an hourly basis, it is observed that the peak value of efficiency and heat gain are 60.58% and 472.47 W. The efficiency enhancement was 3.90% than deionized water. The observation explained that the beam radiation had an influence on solar flux, heat removal factor, collector capacitance factor, and efficiency. On the other side, the overall heat loss is affected by heat loss coefficient and inside heat transfer coefficient for particular receiver material and size. The thermal properties of ambient air, wind velocity, receiver temperature and emissivity of receiver material had an effect on heat loss coefficient.

## References

- [1] Lippke, F., Direct Steam Generation in Parabolic Solar Power Plants: Numerical Investigation of the Transients and the Control of a Once-Through System, *Journal Sol. Energy. Eng.*, 118 (1996), 2, pp. 9-14
- [2] May, E. K., Murphy, L. M., Performance Benefits of the Direct Generation of Steam in Line-Focus Solar Collectors, *Journal Sol. Energy. Eng.*, 105 (1983), 3, pp. 126-133
- [3] Kalogirou, S., Lloyd, S., Use of Solar Parabolic trough Collectors for Hot Water Production in Cyprus, *A Feasibility Study, Renewable Energy*, 2 (1992), 2, pp. 117-124
- [4] Kalogirou, S., Design and Performance Characteristics of a Parabolic-Trough Solar Collector System, *Appl. Energy*, 47 (1994), 4, pp. 341-354
- [5] Vijayan, G., Karunakaran, R., Investigation of Heat Transfer Performance of Nanofluids on Conical Solar Collector under Dynamic Condition, *Adv. Mater. Res.*, 984-985 (2014), July, pp. 1125-1131
- [6] Chaabane, N., et al., Design and Performance of trough Type Solar Collector for Domestic Use, *Proceedings, Symposium on Stirling Cycle.*, Japan, 2014, Vol. 17, pp. 17-20

- [7] Vijayan, G., Karunakaran, R., Experimental Investigation on PTSC Hot Water Generation System, *Journal Adv. Chem.*, 13 (2017), 3, pp. 1-16
- [8] Markus, ECK., Heat Transfer Fluid for Future Parabolic Trough Solar Thermal Power Plants, *Proceedings, 4<sup>th</sup> ISES Solar World Congress on Solar Energy and Human Settlement, Beijing, 2007*, pp. 1806-1812
- [9] Bellos, E., et al., A Detailed Working Fluid Investigation for Solar Parabolic Trough Collector, *Appl. Therm. Eng.*, 11 (2016), Mar., pp. 1-27
- [10] Vikrant Khullar, Himanshu Tyagi, H., Application of Nanofluid as the Working Fluid in Concentrating Parabolic Solar Collectors, *Proceedings, 37<sup>th</sup> National and 4<sup>th</sup> International Conf. on Fluid Mechanics and Fluid Power.*, Chennai, India, 2010, vol. pp.
- [11] Khullar, V., et al., Solar Energy Harvesting Using Nanofluid Based Concentrating Solar Collector, *Proceedings, ASME-3<sup>rd</sup> Micro/Nanoscale Heat and Mass Transfer International Conf.*, Atlanta, Geo., USA, 2012
- [12] Kasaeian, A., et al., Performance Evaluation and Nanofluid using Capability Study of a Solar Parabolic Trough Collector, *Energy Conservation and Management*, 89 (2015), Jan., pp. 368-375
- [13] Li., Q., et al., Experimental Investigation of a Nanofluid Absorber Employed in a Low Profile Concentrated Solar Thermal Collector, *Proceedings, SPIE, Sidney, Australia, 2015, Vol. 9668*
- [14] Ghasemi, S. E., Ranjbar, A., Effect of Nanoparticles in Working Fluid on Thermal Performance of Solar Parabolic Trough Collector, *Journal Mol. Liq.*, 222 (2016), June, pp. 1-31
- [15] Sadaghiyani, O. K., et al., The Effect and Combination of Wind Generated Rotation on Outlet Temperature and Heat Gain of LS-2 Parabolic Trough Solar Collector, *Thermal Science*, 17 (2013), 2, pp. 377-386
- [16] Hachicha, et al., Heat Transfer Analysis and Numerical Simulation of a Parabolic Solar Collector, *Appl. Energy*, 111 (2013), Nov., pp. 583-592
- [17] Wu, Z., et al., The 3-D Numerical Study of Heat Transfer Characteristics of Parabolic Trough Receiver, *Appl. Energy*, 113 (2014), Jan., pp. 902-911
- [18] Coccia, G., et al., Adoption of Nanofluids in Low Enthalpy Parabolic Trough Solar Collectors: Numerical Simulation of the Yearly Yield, *Energy Convers. Manage*, 118 (2016), June, pp. 306-319
- [19] Kaloudis, K., et al., Numerical Simulations of a Parabolic Trough Solar Collector with Nanofluid using Two-phase Model, *Renewable Energy*, 97 (2016), Nov., pp. 218-229
- [20] Natarajan, M., Srinivas, T., Experimental and Simulation Studies on a Novel Gravity based Passive Tracking System for a Linear Solar Concentrating Collector, *Renewable Energy*, 105 (2017), May, pp. 312-323
- [21] Murtuza, S. A., et al., Experimental and Simulation Studies of Parabolic Trough Collector Design for obtaining Solar Energy, *Resour. Effic. Technol.*, 3 (2017), 4, pp. 414-421
- [22] Huang, W., et al., Performance Simulation of a Parabolic Trough Solar Collector, *Sol. Energy*, 86 (2012), 2, pp. 746-755
- [23] Men Wirz, M., Roesle, M., The 3-D, Optical and Thermal, Numerical Model of Solar Tubular Receiver in Parabolic Trough Concentrators, *Journal Sol. Energy Eng.*, 134 (2012), 4, pp. 1-9
- [24] Padilla, R. V., et al., Heat Transfer Analysis of Parabolic Trough Solar Receiver, *Appl. Energy*, 88 (2011), 12, pp. 5097-5110
- [25] De Risi, A., et al., Modelling and Optimization of Transparent Parabolic Trough Collector based on Gas-Phase Nanofluid, *Renewable Energy*, 58 (2013), Oct., pp. 134-139
- [26] Changfu, Y., et al., Modelling of Fluid-Flow and Heat Transfer in Trough Solar Collector, *Appl. Therm. Eng.*, 54 (2013), 1, pp. 247-254
- [27] Valanarasu, A., Sornakumar, S., Theoretical Analysis and Experimental Verification of Parabolic Trough Solar Collector with Hot Water Generation System, *Therm. Science*, 11 (2007), 1, pp. 119-126
- [28] Pavlovic, S. R., et al., Design, Simulation and Optimization of Solar Dish Collector with Spiral Coil Thermal Absorber, *Thermal Science*, 20 (2016), 4, pp. 1387-1397
- [29] Valanarasu, A., Sornakumar, S., Performance Characteristics of the Solar Parabolic trough Collector with Hot Water Generation System, *Thermal Science*, 10 (2006), 2, pp. 167-174
- [30] Stefanovic, V. P., et al., Development and Investigation of Solar Collectors for Conversion of Solar Radiation into Heat and/or Electricity, *Thermal Science*, 10 (2006), 4, pp.177-187
- [31] Vijayan, G., Karunakaran, R., Characteristic Analysis of De-Ionised Water and Ethylene Glycol Based Aluminum Oxide Nanofluid, *Journal Adv. Chem.*, 13 (2017), 5, pp. 6202-6207
- [32] Rashmi, W., et al., Preparation, Thermo-Physical Properties and Heat Transfer Enhancement of Nanofluids, *Mater. Res. Express*, 1 (2014), 032001, pp. 2-48
- [33] Ilyas, S. U., et al., Preparation, Sedimentation and Agglomeration of Nanofluids, *Chem. Eng. and Technol.*, 37 (2014), 12, pp. 2011-2021

- [34] Singh, H., Singh, P., A Review Paper on Performance Improvement of Parabolic trough Collector System, *Journal Appl. Mech. Eng.*, 4 (2015), 2, pp. 1-10
- [35] Kawira1, M., *et al.*, A Prototype Parabolic trough Solar Concentrators for Steam Production, *Journal Agriculture, Sci. Technol.*, 14 (2012), 2, pp. 1-14
- [36] Duffie, J. A., Beckman, W. A., *Solar Engineering of Thermal Processes*, John Wiley and Sons., New York, USA, 2006
- [37] Yogi Goswami, D., *Principles of Solar Engineering*, Taylor and Francis, New York, USA, 2003
- [38] Sukhatme, S. P., *Solar Energy-Principles of Thermal Collection and Storage*, Tata McGraw-Hill Publishing Company Limited., New Delhi, India, 1994
- [39] Vijayan, G., Karunakaran, R., Influence of Dimensionless Parameter on De-ionized Water-Alumina Nanofluid Based Parabolic through Solar Collector, *Recent Patents on NanoTechnology*, 13 (2019), 3, pp. 206-221